measured A/h value appears, if anything, slightly larger than the "octahedral" value. If two H_2O/MnEDTA were actually present the A/h value would be reduced to *ca.* 3×10^6 Hz which seems rather a drastic change. Unlike the Ni(II)–EDTA case where the anomalous temperature dependence of the shift in the $^{17}OH_2$ line indicated the presence (in part) of an unprotonated unbound carboxylate group, the Mn(II) shift behavior is normal for a single species system. The esr results[19] indicating large zero-field splitting also suggest a nonoctahedral structure is present. We conclude that the Mn(II) EDTA–H_2O species is at least seven-coordinate in solution but cannot strictly rule out a higher coordination number at this time. Some preliminary measurements on Mn–EGTA (EGTA is $(O_2CCH_2)_2NCH_2CH_2OCH_2CH_2OCH_2CH_2N(CH_2CO_2^-)_2$) reveal no $^{17}OH_2$ line broadening, consistent with reduced strain in the hexadentate EGTA complex and a total coordination number of six in this complex. More nmr studies of Mn complexes are planned to get more evidence concerning the relations of A/h to structural changes.

Acknowledgments.—This work supported in part by United States Atomic Energy Commission contract AT(45-1)-2221-T4. The assistance of Dr. Grace Y-S Lo in computing matters, and Mr. Thomas Jones for the ir studies is gratefully acknowledged.

CONTRIBUTION FROM THE DEPARTMENT OF CHEMISTRY,
NORTH CAROLINA STATE UNIVERSITY, RALEIGH, NORTH CAROLINA 27607

Magnetic Circular Dichroism Spectra and Electronic Structures of Tris(dialkyldithiocarbamato)chromium(III) Molecules, $Cr(R_2tc)_3$, and Others[1a]

BY A. F. SCHREINER* AND P. J. HAUSER[1b]

Received February 22, 1972

A series of tris(dialkyldithiocarbamato)chromium(III) molecules was studied in d–d regions by means of magnetic circular dichroism, ambient and 80°K electronic absorption, trigonal (D_3) crystal field theory, and ground-state semiempirical LCAO–MO calculations, and some results of the single-crystal X-ray structural analysis of the related $In(pmtc)_3$, where $pmtc^-$ is the pentamethylenedithiocarbamate anion, are given. MCD was found especially well suited for locating the spin forbidden transition $^4A_2 \rightarrow$ "$^2T_2$" and was also reasonably advantageous (over the electronic absorption method) for locating $^4A_2 \rightarrow$ "$^2T_1$." The MCD activity of "$^4T_2$" on the other hand, is weak as in ruby and the individual trigonal components of this state were not detectable in the tc complexes. The large activity of $^2T_2$ permits one to conclude that the order of trigonal components of $^2T_2$ is $^2A_1 < {}^2E$. This ordering and previous publication of the trigonal splitting of $^4T_2(t_2^2e^1)$ as $^4A_1 < {}^4E$ made it possible to carry out a reliable, iterative D_3 crystal field calculation using the variable-secant analog of the Newton–Raphson method by use of an approximate Jacobian. Application of the complete configuration interaction trigonal crystal field model (absence of spin–orbit coupling) led to the conclusion that the use of zero-order theory for obtaining the primary trigonal parameter v, or $|E(^4A_1; T_2) - E(^4E; T_2)| = v_0/2$, would lead to *ca.* 30% underestimate of the absolute value of this parameter when it was compared to the magnitude ($|v_1|$) derived from complete theory for the molecule $Cr(detc)_3$. Interestingly the same discrepancy prevails in $Cr(detp)_3$. However, it was found that the ratio $v_1/v_0 = 1.3$ for both molecules so that the importance of the second trigonal parameter v' is perhaps the same in both compound types. Interestingly the configuration interaction parameter (K') for $Cr(detc)_3$ is numerically about equal to the splitting parameter (K). Also, semiempirical Wolfsberg–Helmholz molecular orbital calculation on the ground state of $Cr(H_2tc)_3$ leads to the conclusion that there is an unexpectedly significant antibonding, across-the-ring Cr–C interaction within the four-membered rings of type i. The data of our series of tc molecules provided no new support for Nakamoto's suggestion that the variation

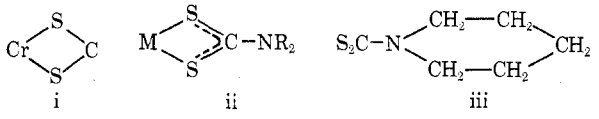

i ii iii

of R in ii will influence the electronic structure of the C–N bond and (our anticipated) subsequent influence on the four-membered ring i. However, the initial single crystal, three-dimensional X-ray structural study of $In(pmtc)_3$ indeed demonstrates such an effect, since the C–N distance of S_2C–N is 0.10 Å less than the C–N distance of the ring in iii. Very important, also, is that the C–N(C)C group is *planar*, which is also consistent with C–N π bonding in the S_2C–N group.

Introduction

MCD studies of D_3 tris bidentate Cr(III) molecules or complex ions have been limited to date to $[Cr(en)_3]^{3+}$ and $[Cr(ox)_3]^{3-}$.[2] We are in the process of studying such D_3 moieties systematically and in detail. This paper reports on the MCD study of the interesting tris(dialkyldithiocarbamato)chromium(III) molecule types, $Cr(R_2tc)_3$, containing the groups

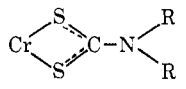

In review, early electronic absorption experiments were carried out on a few such dithiocarbamate (tc) complexes (R = H, ethyl, *n*-butyl) by Kida and Yoneda[3] and Jorgensen,[4] and preliminary *octahedral*

(1) (a) Presented in part at the 162nd National Meeting of the American Chemical Society, Washington D. C., Sept 1971, and in part at the Molecular Structure and Spectroscopy Conference, Columbus, Ohio, June 1971. (b) National Defence Education Association Predoctoral Fellow.

(2) A. J. McCaffery, P. J. Stephens, and P. N. Schatz, *Inorg. Chem.*, **6**, 1614 (1967).

(3) S. Kida and H. Yoneda, *J. Chem. Soc. Jap.*, **76**, 1059 (1955).

(4) (a) C. K. Jorgensen, *J. Inorg. Nucl. Chem.*, **24**, 1571 (1962); (b) C. K. Jorgensen, *Inorg. Chim. Acta Rev.*, **2**, 65 (1968).

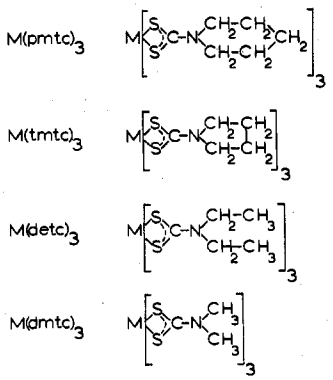

Figure 1.—The four $Cr(R_2tc)_3$ molecules, R_2tc^-: dimethyldithiocarbamate (dmtc), diethyldithiocarbamate (detc), tetramethylenedithiocarbamate (tmtc), pentamethylenedithiocarbamate (pmtc).

crystal field parameters (B, C, Dq, β) were derived. While such studies span the d–d regions ^2E, $^2T_1$, $^4T_2$, $^2T_2$, and $^4T_1$, experimental spin doublet information was sparse. It has since then become possible to locate such weak $^2\Gamma$ bands of $Cr(dmtc)_3$[5] and $Cr(detc)_3$[5] as small shoulders in 4°K unpolarized crystal spectra and 80°K glass spectra[6] and more advantageously as *strong* bands in the solution MCD spectrum of one of these, $Cr(detc)_3$.[6c] Other papers which bear a close relationship to this communication include those of Sugano and Tanabe,[7] Krishnamurthy, Schoop, and Perumareddi,[8] Witzke,[9] and a vibrational analysis paper by Nakamoto, Fujita, Condrate, and Morimoto.[10] Others[11–13] will be brought to light below in the Discussion portion of this paper.

This communication then concerns itself with primarily the MCD properties of the "d–d" states ^2E, $^2T_1$, $^4T_2$, $^2T_2$, and $^4T_1$ of "t_2^3" and "$t_2^2e^1$." The tc series of molecules (tmtc, pmtc, detc, dmtc) of this study is shown in Figure 1. A variation of R was anticipated to be needed in view of the conclusion drawn from vibrational analysis that the amount of C–N multiple bonding depends on the nature of R, and also because when R is H one obtains an unstable complex compared to R = alkyl. We report here conclusions drawn from: (1) MCD spectra, (2) 80°K glass electronic absorption spectra, (3) D_3 crystal field calculations, (4) ground-state semiempirical LCAO–MO calculations, and (5) some data from the single-crystal X-ray study of $In(pmtc)_3$ which is in the completion stage here.

Experimental Section

Instrumental.—The magnetic fields for MCD measurements were generated using a Nb/Ti superconducting coil wound by Westinghouse and built into a 300–80–4°K dewar system. Fields

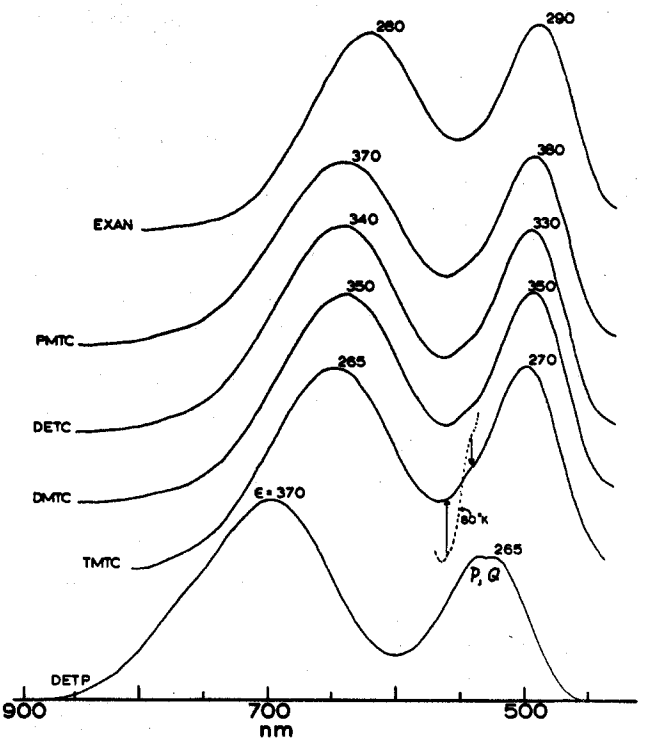

Figure 2.—Ambient and 80°K solution electronic spectra of several $Cr^{III}S_6$ chromophore types.

of *ca.* 42 kG were employed and were measured to within 1% accuracy using a rotating coil gaussmeter. The latter was calibrated against a more accurate Magnion G-502, and the magnetic field and light directions were made to parallel each other. The circularly dichroic light of the Durrum JASCO Model ORD/UV/CD-5 was used, and the xenon source was found not to require shielding in fields used here. However, the end-on photomultiplier tube was removed, shielded, and housed outside the instrument. The instrument is still usable for absorption optical measurements, since the chopper drive cable was lengthened and repositioned by us. The instrument MCD calibration was checked against the spectrum of $K_3[Fe(CN)_6]\cdot 3H_2O$.[2]

The positions of numerous sharp bands of $Nd(NO_3)_3\cdot 5H_2O$, $UO_2(NO_3)_2\cdot 6H_2O$, and silicate glasses of holmium oxide and neodymium oxide (bands between 3000 and 8000 Å) resulted in the following relationship between JASCO and Cary 14 readouts: $\lambda_c = 1.018\lambda_J - 6.003 \times 10^{-5}\lambda_J^2$ where λ_c and λ_J are wavelength (nm) readings on Cary 14 and our JASCO spectrometers.

A Cu–constantan thermocouple and Leeds-Northrup K-3 potentiometer were used to determine the temperatures of the glass samples. Samples were cooled in a quartz exchange-gas dewar.

Sample Handling.—All solid compounds were found to be stable during storage for several months. Solution spectra were obtained using methylene chloride as solvent. The glass spectra were obtained in an EPA–chloroform mixture (8:1 by volume).[6a,b] Normally the glass was found to shatter the optical cell near the end of each experiment.

Preparations.—The ligand salts $Na(tmtc)\cdot 2H_2O$ and $Na(pmtc)\cdot 2H_2O$ were prepared by the method of Gleu and Schwab.[14] The ligand salts $Na(detc)\cdot 3H_2O$ and $Na(dmtc)\cdot 3H_2O$ were purchased from Fisher Scientific Co.

The ligands were complexed with Cr(III) according to the general procedure outlined in the literature.[15] Additional details for the preparations of $Cr(pmtc)_3$ and $Cr(tmtc)_3$ are given since we are unaware of such reports in the literature.

$Cr(pmtc)_3$.—The procedure of ref 15 was followed except that only 0.0275 mol of $CrCl_3$ and 0.075 mol of $Na(pmtc)\cdot 2H_2O$ were used with 200 ml of THF. Thirty minutes after the addition of ligand, the solution was filtered, and the solid residue was treated with 40 ml of $CHCl_3$. The last solution was filtered and the fil-

(5) The abbreviations for dialkylcarbamates are detc = diethyl, dmtc = dimethyl, tmtc = tetramethylene, and pmtc = pentamethylene.

(6) (a) W. J. Mitchell, Ph.D. Thesis, North Carolina State University, 1971; (b) K. DeArmond and W. J. Mitchell, *Inorg. Chem.*, **11**, 181 (1972); (c) P. J. Hauser, A. F. Schreiner, J. D. Gunter, W. J. Mitchell, and M. K. DeArmond, *Theor. Chim. Acta*, **24**, 78 (1972).

(7) (a) S. Sugano and Y. Tanabe, *J. Phys. Soc. Jap.*, **13**, 880 (1958); (b) J. A. Spencer, Ph.D. Thesis, University of Illinois, Urbana, 1970.

(8) R. Krishnamurthy, W. B. Schoop, and J. R. Perumareddi, *Inorg. Chem.*, **6**, 1338 (1967).

(9) H. Witzke, *Theor. Chim. Acta*, **20**, 171 (1971).

(10) K. Nakamoto, J. Fujita, R. A. Condrate, and Y. Morimoto, *J. Chem. Phys.*, **39**, 423 (1963).

(11) J. R. Wasson, S. J. Wasson, and G. M. Woltermann, *Inorg. Chem.*, **9**, 1576 (1970).

(12) A. A. G. Tomlinson, *J. Chem. Soc. A*, 1409 (1971).

(13) J. D. Lebedda and R. A. Palmer, *Inorg. Chem.*, **10**, 2704 (1971).

(14) K. Gleu and R. Schwab, *Angew. Chem.*, **62**, 320 (1950).

(15) F. Galsbol and C. E. Schäffer, *Inorg. Syn.*, **10**, 42 (1968).

trate added to 80 ml of petroleum ether. The blue-violet Cr(pmtc)$_3$ precipitated immediately. The compound was recrystallized twice as previously described.[15] *Anal.* Calcd for Cr(pmtc)$_3$: C, 40.58; N, 7.89; H, 5.68. Found: C, 40.50; N, 8.12; H = 5.90.

Cr(tmtc)$_3$.—The general procedure of ref 15 was followed again except that only 0.0367 mol of $CrCl_3$ and 0.1 mol of Na(tmtc)·$2H_2O$ were used in the 200 ml of THF. The compound was recrystallized twice by the method of ref 15. *Anal.* Calcd for Cr(tmtc)$_3$: C, 36.71; N, 8.56; H, 4.93. Found: C, 36.47; N, 8.34; H, 4.79.

While this compound was stable in the solid state, we observed that solutions of it slowly decomposed. For example, extinction coefficient ϵ_{max} of $^4T_2$ decreased about 5% in 24 hr, and it became possible to separate out elemental sulfur. The decomposition was insignificant during spectral measurements. Interestingly this was the only tc molecule of the four which underwent such an oxidation step. We are in the process of studying this interesting molecule by several other means.

Results

The coordinated tc ligand molecules, dimethyldithiocarbamate (dmtc), diethyldithiocarbamate (detc), tetramethylenedithiocarbamate (tmtc), and pentamethylenedithiocarbamate (pmtc), are shown in Figure 1. The electronic spectra of the four tc complexes make up Figure 2 along with those of the similar tris(ethyl xanthato)chromium(III) (Cr(exan)$_3$) and tris(diethyl dithiophosphato)chromium(III) (Cr(detp)$_3$). The 80°K glass spectra contain additional structure in the region between $^4T_1$ and $^4T_2$ as shown in Figures 2 and 3. Electronic absorption band locations (Cary 14) at *RT* and 80°K are given in Table I. The MCD

TABLE I
BAND EXTREMA[c] OF CHROMIUM(III) DITHIOCARBAMATES

	Electronic absorption				
	RT	80°K	Ref 4	MCD	Assignments
Cr(tmtc)$_3$	499	499		494	$^4E(^4T_1)$
	(534)	(545)		519, 541	$^2E(^2T_2)$
		(560)		(553)	$^2A_1(^2T_2)$
	648	638		(646)	$^4T_2$
				728	$^2T_1$
				~775	^2E
	492	494		490	$^4E(^4T_1)$
Cr(pmtc)$_3$	(535)	(546)		519, 544	$^2E(^2T_2)$
	641	630		655	$^4T_2$
				739	$^2T_1$
				~770	^2E
Cr(dmtc)$_3$	493		493[a]	486	$^4E(^4T_1)$
	(533)		540[a]	517, 541	$^2E(^2T_2)$
	(547)		551[a]		$^2A_1(^2T_2)$
	641		630[a]	646	$^4T_2$
				725	$^2T_1$
				~775	^2E
Cr(detc)$_3$	496		493[b]	479	$^4E(^4T_1)$
	(533)		540[b]	519, 543	$^2E(^2T_2)$
	(547)		549[b]		$^2A_1(^2T_2)$
	644		645[b]	646	$^4T_2$
				730	$^2T_1$
			760[b]	~775	^2E

[a] 4°K unpolarized crystal spectrum. [b] 80°K glass spectrum. [c] $\lambda_{Cary} = 1.018\lambda_{JASCO} - 6.003 \times 10^{-5}\lambda_{JASCO}^2$.

spectra (JASCO) of the four tc molecules in methylene chloride constitute the substance of Figure 4. (Note that the two lowest energy extrema a and b are intense compared to c and d. This was observed to occur for each of the four tc molecules.) The higher energy MCD regions ($^4T_1$, $^2T_2$) are most interesting, and the

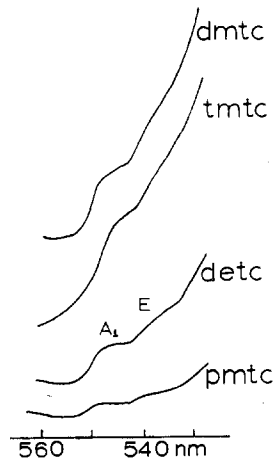

Figure 3.—Solution spectra (80°K) of A_1 and E of $^2T_2$.

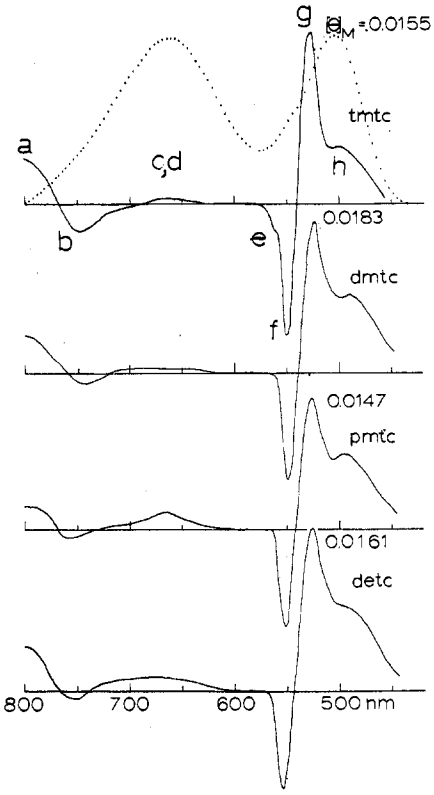

Figure 4.—Solution MCD spectra of four Cr(tc)$_3$ molecules.

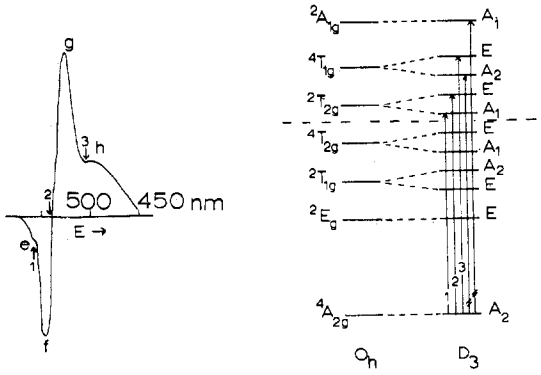

Figure 5.— The $^2T_2$, $^4T_1$ MCD region of Cr(tmtc)$_3$ and order of trigonal states.

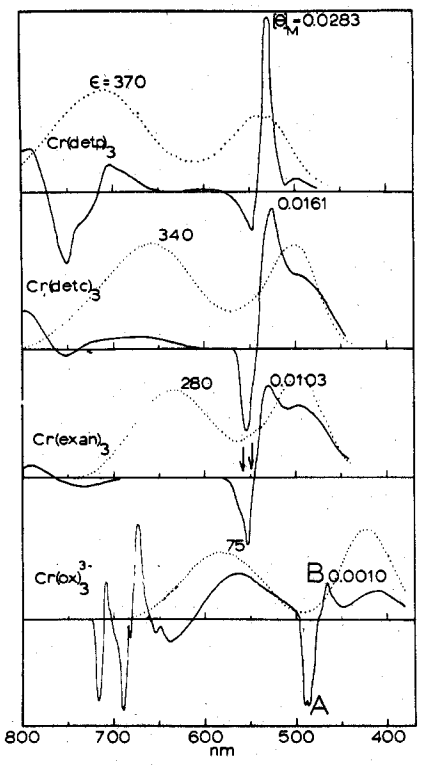

Figure 6.—Comparative MCD spectra of $Cr(detp)_3$, $Cr(detc)_3$, $Cr(exan)_3$, and $Cr(ox)_3^{3-}$. The two arrows in the $Cr(exan)_3$ spectrum point to the locations of ^2A and ^2E of $^2T_2$ observed at 80°K, with the molecule in a methyl methacrylate matrix.[6b]

tmtc spectrum is best resolved of the four. Labels e, f, g, h of Figure 5 refer to MCD extrema, and arrows in the spectrum point to electronic absorption band maxima. The assignments for the high-energy region of tmtc are also shown in Figure 5. It is to be noted here that whereas there are only three orbitally allowed trigonal states (^2E, $^2A_1$, ^4E) in this region, we find four MCD extrema (e–h) as in tmtc. Figure 6 permits a comparison of trigonal MCD features of the

TABLE II

ENERGY LEVELS IN $Cr(detc)_3$

Obsd bands, cm^{-1}	Calcd bands, cm^{-1}	Assignments
12,930	12,900	$^2E(E_g)$
13,610	13,640	$^2E(T_{1g})$
15,150[a]	15,150	$^4A_1(T_{2g})$
15,950[a]	15,950	$^4E(T_{2g})$
18,280	18,280	$^2A_1(T_{2g})$
18,620	18,620	$^2E(T_{2g})$
20,000	20,000	$^4E(T_{1g})$

Parameters, cm^{-1}

Dq	1562	v	−2131
B	335	v'	−745
$C(^2E_g)$	3666	K	710
$C(^2T_{1g})$	3527	K'	−745
$C(^2T_{2g})$	3063		

[a] Reference 12.

TABLE III

SENSITIVITY OF COMPUTED ENERGY LEVELS (cm^{-1}) TO CRYSTAL FIELD PARAMETERS (cm^{-1}): $Cr(detc)_3$

	Dq	B	$C(^2E_g)$	$C(^2T_{1g})$	$C(^2T_{2g})$	v	v'
$^2A_1(T_{2g})$	1.153	10.640	0.000	0.000	4.143	−0.027	−0.254
$^4A_1(T_{2g})$	9.965	−0.053	0.000	0.000	0.000	0.000	0.549
$^2E(E_g)$	0.104	8.206	1.333	1.362	0.469	0.589	−0.170
$^2E(T_{1g})$	0.024	7.961	1.450	1.538	0.015	−0.012	−0.117
$^2E(T_{2g})$	1.233	9.108	0.279	0.099	3.665	−0.648	0.458
$^4E(T_{2g})$	9.949	0.639	0.000	0.000	0.000	−0.269	0.544
$^4E(T_{1g})$	10.325	8.766	0.000	0.000	0.000	−0.746	0.896

TABLE IV

ENERGY LEVELS IN $Cr(detp)_3$

Calcd and obsd bands, cm^{-1}	Assignments	Calcd and obsd bands, cm^{-1}	Assignments
13,010	$^2E(E_g)$	17,400	$^2A_1(T_{2g})$
13,590	$^2E(T_{1g})$	18,750	$^2E(T_{2g})$
13,860[a]	$^4A_1(T_{2g})$	19,250	$^4E(T_{2g})$
14,500[a]	$^4E(T_{2g})$		

Parameters, cm^{-1}

Dq	1319	v	−1674
B	386	v'	840
$C(^2E_g)$	3553	K	558
$C(^2T_{1g})$	3497	K'	840
$C(^2T_{2g})$	2929		

[a] Reference 13.

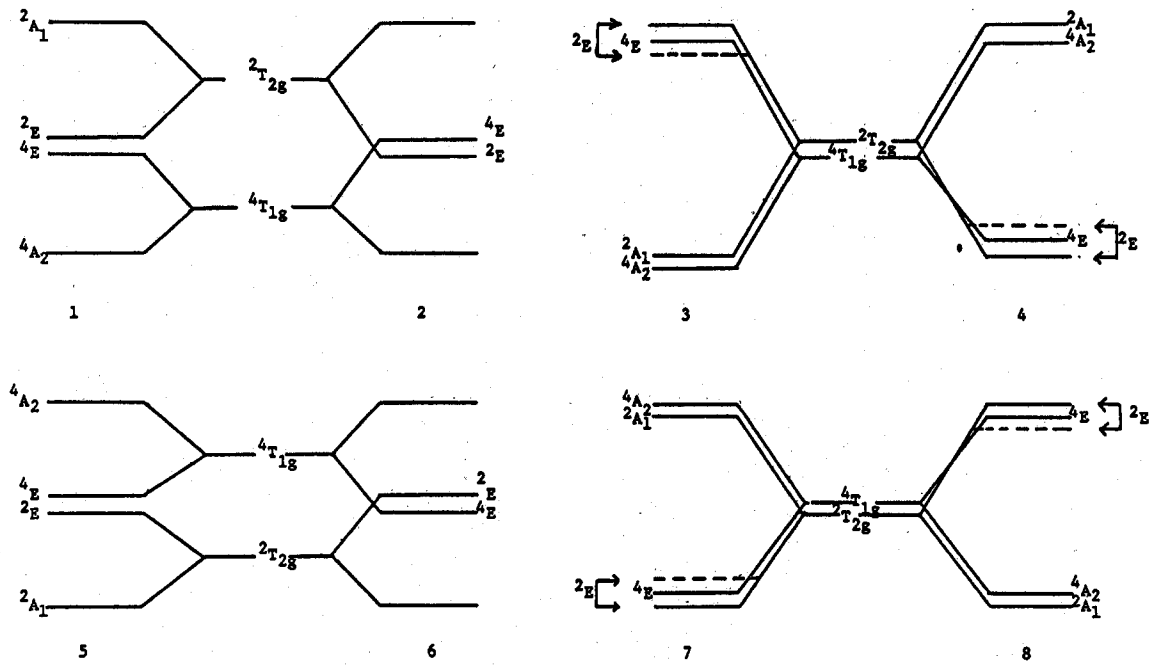

Figure 7.—The numerous possible orders of trigonal components of $^2T_2$ and $^4T_1$ for either case $^2T_2 > {}^4T_1$ or $^2T_2 < {}^4T_1$.

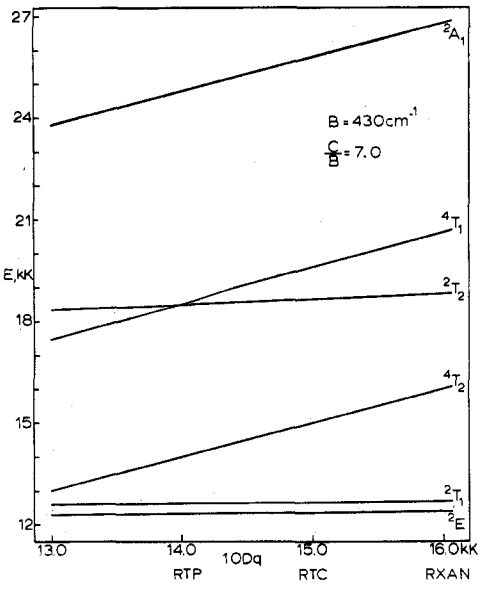

Figure 8.—The approximate positions of octahedral $Cr(R_2tp)_3$, $Cr(R_2tc)_3$, and $Cr(Rxan)_3$ energies *vs.* Dq.

TABLE V

SENSITIVITY OF COMPUTED ENERGY LEVELS (cm^{-1}) TO CRYSTAL FIELD PARAMETERS (cm^{-1}): $Cr(detp)_3$

	Dq	B	$C(^2E_g)$	$C(^2T_{1g})$	$C(^2T_{2g})$	v	v'
$^2A_1(T_{2g})$	1.695	8.735	0.000	0.000	4.110	−0.021	−0.325
$^4A_1(T_{2g})$	9.965	−0.037	0.000	0.000	0.000	0.000	0.867
$^2E(E_g)$	0.330	7.239	2.254	0.443	0.507	0.618	−0.104
$^2E(T_{1g})$	0.215	7.570	0.548	2.414	0.020	0.011	−0.179
$^2E(T_{2g})$	1.190	9.715	0.251	0.146	3.567	−0.678	0.510
$^4E(T_{2g})$	9.992	0.270	0.000	0.000	0.000	−0.316	0.809
$^4E(T_{1g})$	10.178	9.610	0.000	0.000	0.000	−0.700	1.126

TABLE VI

COMPARISON OF PARAMETERS (cm^{-1})

Parameter	$Cr(detp)_3$	$Cr(detc)_3$	Parameter	$Cr(detp)_3$	$Cr(detc)_3$
Dq	1319	1562	v	−1674	−2131
B	386	335	v'	840	−745
$C(^2E_g)$	3553	3666	K	558	710
$C(^2T_{1g})$	3497	3527	K'	840	−745
$C(^2T_{2g})$	2928	3063			

TABLE VII

ENERGY LEVELS IN $Cr(detc)_3$ (SIX-PARAMETER MODEL)

Obsd bands, cm^{-1}	Calcd bands, cm^{-1}	Assignments
12,930	12,850	$^2E(E_g)$
13,610	13,720	$^2E(T_{1g})$
15,150	15,150	$^4A_1(T_{2g})$
15,950	15,950	$^4E(T_{2g})$
18,280	18,280	$^2A_1(T_{2g})$
18,620	18,612	$^2E(T_{2g})$
20,000	20,000	$^4E(T_{1g})$

Parameters, cm^{-1}			
Dq	1562	v	−2131
B	335	v'	−745
$C(^2E_g) = C(^2T_{1g})$	3600		
$C(^2T_{2g})$	3063		

$Cr^{III}S_6$ chromophore of several ligands with the CrO_6 chromophore, *i.e.*, as in $[Cr(ox)_3]^{3-}$, also reported by McCaffery, *et al.*[2]

Figure 7 qualitatively demonstrates numerous possible orders of D_3 states for either $^2T_2 > {}^4T_1$ or $^2T_2 < {}^4T_1$, and Figure 8 shows the approximate positions of various CrS_6 chromophores on an octahedral crystal field diagram of energy *vs.* Dq for $C/B = 7$ and $B = 430$ cm^{-1}.

Tables II and III summarize experimental and calculated data for $Cr(detc)_3$. Analogous data make up Tables IV and V for $Cr(detp)_3$, and Table VI is a comparison of crystal field parameters for these two molecules. Finally, Table VII demonstrates that the seven-band fit was also achieved using a six-parameter trigonal crystal field model.

Discussion

The general and expected features (Figure 2) of the electronic absorption spectra of the tc complexes of Figure 1 are that transitions $^4A_2 \rightarrow {}^4T_2$ (~650 nm) and $\rightarrow {}^4T_1$ (~500 nm) dominate the intensities in these molecules. However, at about 535 nm in every spectrum (Figure 3) there is a small shoulder even at room temperature. At 80°K a second small band appears (Figures 2, 3) at *ca.* 545 nm because $^4T_1$ narrows considerably, and these two bands of very low intensity (with $\epsilon < 1$) are reasonably assigned to the two trigonal components of $^2T_2$ ($^2A_1$, ^2E). However, the order cannot be determined at this stage, but it will be established as described below. We mention at this point that low-intensity structure in these regions was also observed[6a,b] in the unpolarized crystal spectra of detc and dmtc complexes. The other two ^2T components, $^2E(E)$ and $^2E(T_1)$, were anticipated to show up (Figure 8) on the red side of $^4T_2$ but were not observed at 80°K in electronic spectra, but MCD advantageously reveals these bands (*vide infra*), as do methyl methacrylate pellets.[6a]

The low-energy region with $^2E(E)$ and $^2E(T_1)$, bands a and b, between 700 and 800 nm of tc complexes were found to have fairly high MCD activity (Figure 4) with H = 40,000 G. However, the JASCO is least accurate in this region as far as the intensities of the lowest energy band of each compound is concerned. The 650-nm region of $^4T_2$ (band c + d, Figure 4) is noticeably of very low intensity for each of the tc compounds similar to ruby which has also been found to have little if any activity in this $^4T_2$ state.[7b] We are continuing to investigate the cause of this characteristic in the tc molecules, but the origin is probably related to smallness of C terms at the high temperature of 300°K.

We now move on to the high-energy MCD region ($^2T_2$, $^4T_1$) of these compounds, which is the primary topic of this paper. This region of CrS_6 systems has been somewhat controversial, *e.g.*, electronic absorption bands P and Q in $Cr(detp)_3$ (Figure 2) have previously been attributed to the D_3 components of $^4T_1$ since they are both intense;[11] but also, P and Q have been associated with $^4T_1$ and $^2T_2$, respectively,[12,13] and also with $^2T_2$ (P) and $^4T_1$ (Q).[6a,c] The close proximity of $^2T_2$ and $^4T_1$ is largely responsible for the differences in interpretation, and the situation can give rise to numerous trigonal orders (Figures 7, 8). We propose to establish the correct order.

It might be noted first that the MCD activity in general of the tc molecules is very high (Figures 4, 5, 6) in this region, and f and g are very sharp bands. Also, our earlier dilemma for $Cr(detp)_3$ of observing four MCD extrema (e, f, g, h) but expecting only three spatially allowed states (^2E, $^2A_1$, ^4E) can now be understood (*vide infra*).

$Cr(tmtc)_3$ gave the best resolved high-energy MCD spectrum (Figures 4, 5). The three arrows of Figure 5

point to the positions of the three electronic absorption band maxima, the lower two to $^2T_2$ components and the highest to $^4E(T_1)$. The lowest energy MCD band in this region is relatively very weak and apparently of $(B + C)$-term character, as the electronic and MCD extrema coincide. Also, ^4E at highest energy (band h) appears to be mostly of B-term composition. The middle band 2 (Figure 5) is most interesting. Note that this electronic absorption band is very near the cross-over node of the MCD dispersion, which is *apparently* a positive A term with very little $B + C$ feature. However, we experimentally estimate $A/D \approx 40$ BM (D = dipole strength) from either a Gaussian analysis or form the equivalent extremum formula

$$[\theta]^{A(a\rightarrow j)}_{M,max} = \left(\frac{24NH}{\hbar c}\right) \times \left[\frac{\sqrt{\pi}\nu_0}{\sqrt{2eh}\Delta_0^2} + \frac{\sqrt{\pi}}{2\sqrt{eh}\Delta_0}\right] A(a\rightarrow j) \quad (1)$$

where $[\theta]_{M,max}$ is *half* the peak to trough ellipticity. (For other quantities refer to ref 16.)

Since the magnitude of this A term is much larger than expected, f + g cannot be a true A term. Instead, it is a pseudo A term composed of primarily two overlapping $(B + C)$ terms of opposite signs but of about the same magnitude. Their origin must be the closely spaced Kramer's $2\bar{A}$ and $\bar{E}_a$ of $^2E(T_2)$. Thus their close spacing could result in very large B terms, but the ground state could make a large B contribution as well, *e.g.*, for the transition $\bar{E}(a) \rightarrow \bar{E}_a$, or $a \rightarrow j$.

$$B(a\rightarrow j) \simeq \mathrm{Im}\left[\frac{\langle 2\bar{A}(a)|\hat{u}|E(a)\rangle}{\Delta E[2\bar{A}(a) - \bar{E}(a)]} \cdot \langle \bar{E}(a)|\widehat{eq}|\bar{E}_a\rangle \times \langle \bar{E}_a|\widehat{eq}|2\bar{A}(a)\rangle + \frac{\langle \bar{E}_a|\hat{u}|2\bar{A}\rangle}{\Delta E[2\bar{A}(a) - \bar{E}_a]} \cdot \langle \bar{E}(a)|\widehat{eq}|\bar{E}_a\rangle \times \langle 2\bar{A}|\widehat{eq}|\bar{E}(a)\rangle\right] \quad (2)$$

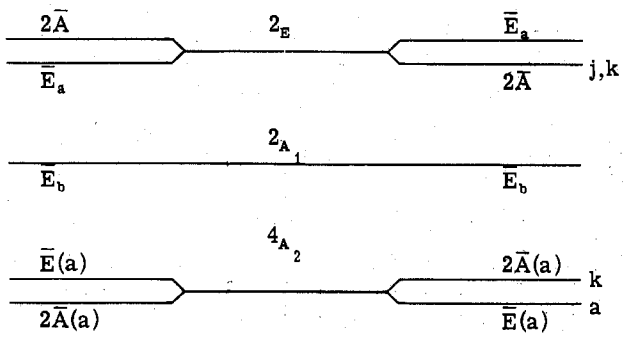

A similar expression could be written for the second component, $\bar{E}(a) \rightarrow 2\bar{A}$, except the sign of ΔE in the second term would reverse. Bands f and g may also have large C character in their intensities. Thus our band assignments for $Cr(tmtc)_3$ and the other tc complexes are the following: e, $^2A_1(^2T_{2g})$; f, g, $^2E(^2T_{2g})$; and h, $^4E(^4T_{1g})$. Furthermore, from Tomlinson's[12] polarized crystal result of the $^4T_{2g}$ region of $Cr(detc)_3$, it is known that $^4E > {}^4A_1$ (both of $^4T_{2g}$).

This knowledge combined with the $^2T_{2g}$ information ($^2E > {}^2A_1$) permit one to carry out a reliable trigonal crystal field calculation with B, C, Dq, and the trigonal field parameters v and v' to be found, since the one electron operator is[17] (see Appendix I)

$$V_{trig} = 10Dq\left[-\frac{1}{5}\sqrt{70}Y_4^0 - 2(Y_4^3 - Y_4^{-3})\right] - v\left[\frac{1}{7}\sqrt{70}Y_2^0 - \frac{4}{21}\sqrt{70}Y_4^0 + \frac{2}{3}(Y_4^3 - Y_4^{-3})\right] + v'\left[\frac{4}{7}\sqrt{35}Y_2^0 + \frac{4}{7}\sqrt{35}Y_4^0 - \sqrt{2}(Y_4^3 - Y_4^{-3})\right] \quad (3)$$

We used Perumareddi's[18] strong field matrix elements, including configuration interaction, and made the calculation compatible with the secant variant of the Newton–Raphson solution seeking method[19] (see Appendix II). For best fits we found it necessary to allow for different values of Racah C parameters, *viz.*, one each of ^2E_g, $^2T_{1g}$, $^2T_{2g}$ as suggested by Witzke recently.[9] The theory also works with $C(^2E_g) = C(^2T_{1g}) \neq C(^2T_{2g})$ (see Table VII).

The numerical results for $Cr(detc)_3$ are given in Table II. First, zero-order trigonal theory leads one to conclude that v is negative because $^4E > {}^4A_1$ for $^4T_2$. Indeed both parameters v and v' were negative even after treating the data with complete strong field, configuration interaction theory (Table II). However, zero-order theory ($v = -1600$ cm^{-1}) underestimates the magnitude of v ($v = -2131$ cm^{-1}).

A second point of interest is the large C/B ratio, $9 \lesssim (C/B) \lesssim 11$, a point recognized from O_h calculations.[6c,13]

Third, the configuration interaction parameter K' is quite large (-745 cm^{-1}), as is the trigonal splitting parameter K (710 cm^{-1}). Fourth, the nephelauxetic ratio $\beta = 0.325$ is small, which is an indication of extensive electron delocalization. Our ratio $C_{(av)}/C_{F.I.} = 0.896$.

The sensitivity of band positions to numerical changes of the crystal field parameters is given in Table III. From it one can see that the position of each band is most sensitive to either B or Dq, but $^4E(T_{1g})$ is sensitive to both parameters. Finally, we conclude that the $^2T_{2g}$ trigonal components are more "delocalized" than either the $^2T_{1g}$ or ^2E_g components on the basis of the numerical values of C parameters, *i.e.*, $C(^2T_{2g}) < C(^2T_{1g}) \approx C(^2E_g)$. On using the slightly different band positions of ref 6b for $^2E(E)$ and $^2E(T_1)$, only parameters $C(^2T_1) = 3722$ cm^{-1} and $C(^2E) = 3576$ cm^{-1} take on somewhat different values.

In view of the great similarities of electronic and MCD spectra among the four tc complexes, we make the same assignments for all four tc compounds. Furthermore, due to the very strong resemblance of the electronic and MCD spectra of $Cr(exan)_3$ (exan = ethyl xanthate, $S_2COC_2H_5$) to the spectra of the tc series, we assign the electronic transitions of $Cr(exan)_3$ similarly.

We now turn our attention to $Cr(detp)_3$. There are two excellent reasons for assigning the high energy state order as $^2A_1(T_{1g}) < {}^2E(T_{1g}) < {}^4E(T_{1g})$, *i.e.*, in the same sequence as in $Cr(detc)_3$. First, the molecule has

(16) P. J. Stephens, W. Suëtaak, and P. N. Schatz, *J. Chem. Phys.*, **44**, 4592 (1966).

(17) R. M. MacFarlane, *J. Chem. Phys.*, **39**, 3118 (1963).

(18) J. R. Perumareddi, *J. Phys. Chem.*, **71**, 3144 (1967).

(19) C. E. Fröberg, "Introduction to Numerical Analysis," Addison-Wesley, Reading, Mass., 1965, p 19.

a very small ($\epsilon \sim 1$) electronic absorption band near 17.4 kK which is reasonably assigned to the lowest energy D_3 component of $^2T_{1g}$. Second, the features of MCD extrema f–g–h closely resemble those of the tc compounds. For this reason we assign MCD bands f and g to $^2E(T_{2g})$ (electronic absorption maximum P occurs close to the MCD node of f and g). We further add that polarized crystal studies also identified band P as being of E symmetry,[12,13] but the data did not distinguish between ^4E and ^2E. The small MCD activity in $^4E(T_{2g})$ appears to be a consequence of mutual cancellation of MCD intensities in bands f and h. The activity near 17.4 kK is associated with the $^2A_1$ component of $^2T_{2g}$ since the ^2E component has already been assigned. Thus, after choosing band positions as identified in Table IV an accurate D_3 crystal field calculation can be carried out in the same manner as before. The results are summarized in Table IV.

Table V contains the sensitivity of calculated band positions of $Cr(detp)_3$ to variations in the crystal field parameters. Dq and B are the most sensitive parameters as was found for $Cr(detc)_3$. The comparison of crystal field parameters for the two molecules $Cr(detc)_3$ and $Cr(detp)_3$ is best made by referring to Table VI. For example, the latter compound clearly has the smaller Dq value, whereas parameter v is larger for $Cr(detc)_3$. Also in $Cr(detp)_3$ as in $Cr(detc)_3$, $^2T_{2g}$ is more "delocalized" than either $^2T_{1g}$ or ^2E_g.

We now turn to Figure 6 for the comparison of CrS_6 molecules and $[Cr(ox)_3]^{3-}$.[2] It can be noted immediately that the $^2T_2$, $^4T_1$ region of CrS_6 has ~ 10 times the MCD activity of $[Cr(ox)_3]^{3-}$ when a number of extrema are compared. $^4E(T_{2g})$ of every $Cr(tc)_3$ molecule has positive ellipticity, which is also true of the net $^4T_{1g}$ activity of every compound. Furthermore, the MCD region A–B of $[Cr(ox)_3]^{3-}$ strongly resembles the MCD activity of the three CrS_6 systems in the $^2E(T_{2g})$ regions near 550 nm (also labeled f–g in Figure 4). We tentatively assign A–B to $^2E(T_2)$ of $[Cr(ox)_3]^{3-}$. However, the location of $^2A_1(T_{2g})$ is not known, and the MCD dispersion of ^2E, $^2T_{1g}$ is too complex to lend itself to interpretation at this time.

In passing we point out that a ground state, single determinant Wolfsberg–Helmholz LCAO–MO calculation gives some insight into the relative atom–atom overlap populations, indicative of relative bond orders, in these trigonal tc and tp complexes. Figure 9 summarizes these quantities for $Cr(H_2tp)_3$ and $Cr(H_2tc)_3$. We find that in both compounds there is an across-thering antibonding interaction with a Cr–P or Cr–C overlap population of ~ -0.20. In the case of $Cr(H_2tp)_3$ this is largely a consequence of 4s and 4p orbitals of Cr interacting with 3s and 3p orbitals of P, *i.e.*, overlap integrals between 3d Cr and 3d, 3s, and 3p P orbitals are comparatively small. This predicted interaction is probably reasonable in view of the unusually large V–^{31}P hyperfine interaction constant observed in the esr spectrum of very similar molecules like $V(detp)_3$.[20] The other interesting feature is that the Cr–S overlap population is much smaller than the S–C value, which is consistent with the use of crystal field theory for understanding the d–d transitions of both tc and tp complexes.

Finally, one can conclude that separations of ground

(20) J. R. Wasson, *Inorg. Chem.*, **10**, 1531 (1971).

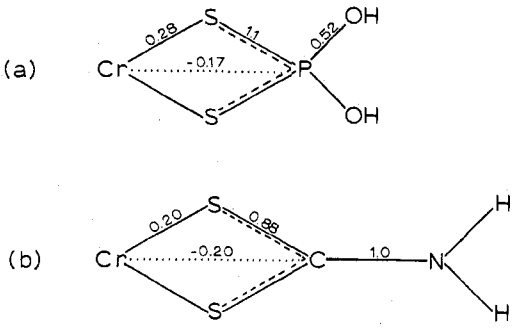

Figure 9.—Atom–atom Mulliken overlap populations in $Cr(H_2tp)_3$ (a) and $Cr(H_2tc)_3$ (b).

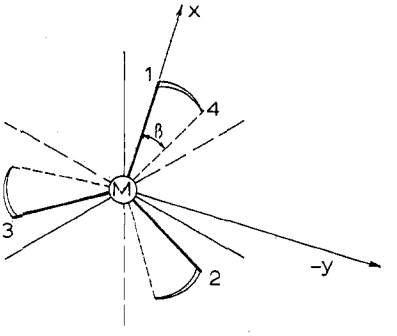

Figure 10.—A coordinate system of a general trigonally distorted, six-coordinate molecule ML_6 looking down C_3 axis (Z axis). Angle β is the projection of chelate angle L_1–M–L_4 into the xy plane, the plane of the paper (see Appendix I).

and electronic excited states do not vary significantly in the series of tc molecules studied (see Table I). However, in order to ascertain whether or not there is multiple bonding between C–N of

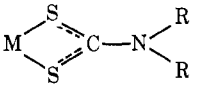

and to characterize the angles in the six-atom moiety

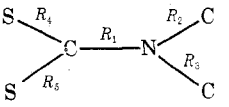

a single-crystal X-ray study was begun on $In(pmtc)_3$. The interesting conclusions thus far are that (1) R_1 is shorter than R_2 by 0.10 Å ($R_3 = R_2$), which is indeed indicative of multiple bonding, (2) the six-atom moiety is *planar*, and (3) the pmtc molecule bonds symmetrically to In(III) because $R_4 = R_5$. The first two conclusions are consistent with Nakamoto's C–N multiple bonding hypothesis of other such tc complexes.[10] The fully detailed report of this structural determination will be issued upon its completion.[21]

Acknowledgments.—Computer calculations were carried out on the IBM 370/165 of the Triangle Universities Computation Center (TUCC). We thank the School of Physical and Mathematical Sciences of this University for liquid helium funds.

Appendix I

The total crystal field operator, V_{trig}, of the six-coordinate trigonal field of six equivalent ligands has in

(21) P. J. Hauser, J. Bordner, and A. F. Schreiner, submitted for publication.

the past been expressed in several forms. Thus it can be written either in operator form with both $[r_<^k/r_>^{k+1}]$ and $\mathbf{Y}_n^l$ as operators or, since V is a one-electron operator, in operator-parameter form, with $\mathbf{Y}_n^l$ the operator but the "radial" portion (ligand coordinates and $\langle r_<^k/r_>^{k+1}\rangle$ as parameters (v, v'; K, K'; Ds, Dt; etc.). The explicit form of V also depends on the choice of the molecular coordinate system. With the coordinate system of Figure 10 we derive V_{trig} in operator form[22]

$$V_{trig} = eq\left(\frac{r^2}{R^3}\right)6\sqrt{\frac{\pi}{5}}(3\cos^2\alpha - 1)\mathbf{Y}_2^0 + eq\left(\frac{r^4}{R^5}\right)\frac{3\sqrt{\pi}}{2}\left(\frac{35}{3}\cos^4\alpha - 10\cos^2\alpha + 1\right)\mathbf{Y}_4^0 + eq\left(\frac{r^4}{R^5}\right)\sqrt{35\pi}\left[\sin^3\alpha\cos\alpha\sin\left(\frac{3}{2}\beta\right)\right](\mathbf{Y}_4^{-3} - \mathbf{Y}_4^3)$$

Here all variables appear as operators, β is the projection of the chelate angle (L_1–M–L_4) in the xy plane, and α is the angle between the C_3 axis and the M–L_1 vector. This form is very useful since it shows that the operator must have "azimuthal" dependence (β) as well as polar dependence (α). Indeed, V of eq 3, which is written in one-electron integral form, is appropriate because it contains parameters v and v', *viz.*

$$v = -3\left[-\frac{3}{7}(3\cos^2\alpha - 1)\langle R_2\rangle - \frac{5}{21}\left(\frac{35}{3}\cos^4\alpha - 10\cos^2\alpha + 1\right)\langle R_4\rangle - \frac{5\sqrt{2}}{9}\left(\sin^3\alpha\cos\alpha\sin\left(\frac{3}{2}\beta\right)\right)\langle R_4\rangle\right]$$

and

$$v' = \frac{3\sqrt{2}}{7}(3\cos^2\alpha - 1)\langle R_2\rangle - \frac{5\sqrt{2}}{28}\left(\frac{35}{3}\cos^4\alpha - 10\cos^2\alpha + 1\right)\langle R_4\rangle - \frac{5}{6}\left(\sin^3\alpha\cos\alpha\sin\left(\frac{3}{2}\beta\right)\right)\langle R_4\rangle$$

where $R_k = \langle R_n^k|r_<^k/r_>^{k+1}|R_n^k\rangle$. Thus v and v' are dependent on both angles α and β. The deletion of the β dependence from the trigonal six-coordinate Hamiltonian may lead to significant discrepancy between crystal field theory and experiment.[23]

Appendix II

It was found that the trial and error approach for finding the crystal field parameters was computationally and man-hour wise rather undesirable, especially since the number of experimental bands was relatively large.

(22) P. J. Hauser and A. F. Schreiner, details on new formalism to be submitted for publication.

(23) A. B. P. Lever and B. R. Hollebone, *J. Amer. Chem. Soc.*, **94**, 1816 (1972).

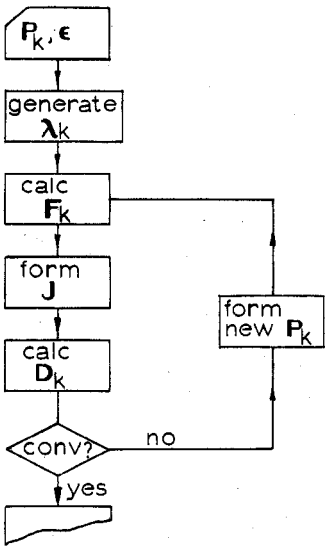

Figure 11.—Flow diagram of presently used variable-secant analog of Newton–Raphson method (see Appendix II).

In the situation here the number of parameters to be extracted was that of the number of observed transitions, so that we proceeded to adapt the variable-secant analog to the Newton–Raphson method for finding the solutions (see ref 19). Since this approach should have general utility, we state its essence here. The equations used are

$$\mathbf{J}_{(K-1,\,K)}{}^{(n,n)}\mathbf{D}_K{}^{(n,1)} = -\mathbf{F}_K{}^{(n,1)} \quad \text{(a)}$$

$$\mathbf{P}_{K+1}{}^{(n,1)} = \mathbf{P}_K{}^{(n,1)} + \mathbf{D}_K{}^{(n,1)} \quad \text{(b)}$$

$$\mathbf{F}_K = \boldsymbol{\lambda}_K - \boldsymbol{\varepsilon} \quad \text{(c)}$$

$$J(i,j) = \frac{\lambda_i(P_1{}^K, \ldots, P_j{}^K, \ldots, P_n{}^K) - \lambda_i(P_1{}^K, \ldots, P_j{}^{K-1}, \ldots, P_n{}^K)}{[P_j{}^K - P_j{}^{K-1}]} \quad \text{(d)}$$

λ_i is the ith energy calculated with the parameter set defined by the contents of the parentheses, $\boldsymbol{\lambda}_K$ is the computed array using $\mathbf{P}_K$, $\mathbf{F}_K$ is the energy error matrix using the Kth parameter set of $\mathbf{P}_K$, $\mathbf{D}_K$ is the increment array which modifies $\mathbf{P}_K$ to give the new parameter array $\mathbf{P}_{K+1}$, and $\mathbf{J}$ is the approximate Jacobian. The process is easily machine adaptable by the following steps. First, two initial parameter arrays $\mathbf{P}_{K-1}$ and $\mathbf{P}_K = \mathbf{P}_{K-1} + 0.05\mathbf{P}_{K-1}$ are assumed based on a set of parameters having reasonable magnitudes. Next, $\boldsymbol{\lambda}_K$ is obtained using $\mathbf{P}_K$ and the crystal field equations, and $\mathbf{F}_K$ is generated from eq b, $\mathbf{F}_K = \boldsymbol{\lambda}_K - \boldsymbol{\varepsilon}$. $\mathbf{J}_{(K-1,\,K)}$ can be obtained using $\mathbf{P}_K$ and $\mathbf{P}_{K-1}$ (eq d). This $\mathbf{J}$ and the above $\mathbf{F}_K$ are used in eq a to find $\mathbf{D}_K$ using IBM's SIMQ of SSP. A convergence test can now be carried out. If the computed energies are not close enough to observed ones, a new cycle is begun by constructing a new parameter array, $\mathbf{P}_{K+1}$ from $\mathbf{P}_K$ and $\mathbf{D}_K$ witn eq b. In the machine procedure the new $\mathbf{P}_{K+1}$ becomes $\mathbf{P}_K$, $\mathbf{P}_K$ becomes $\mathbf{P}_{K-1}$, etc. The flow diagram is shown in Figure 11.